Factors Affecting Laboratory Rutting Evaluation of Airport Pavement Granular Layers

Erol Tutumluer & In Tai Kim
Department of Civil and Environmental Engineering, University of Illinois, Urbana, Illinois, USA

ABSTRACT: This paper presents research findings on characterizing and predicting the permanent deformation behavior of airport pavement granular base/subbase layers constructed and tested at the National Airport Pavement Test Facility (NAPTF) in the United States. The P209/P154 aggregate materials were used in the construction and testing of the NAPTF flexible pavement test sections with variable thickness base and subbase courses. To account for the rutting performances of these substantially thick granular layers, a comprehensive set of repeated load triaxial tests were conducted in the laboratory on the P209 base and P154 subbase granular materials. Based on the laboratory test results, mathematical models were developed to predict maximum permanent deformations occurred under both 6-wheel and 4-wheel gear loadings applied following a wander pattern. The performances of the developed rutting models were evaluated for predicting the field accumulation of permanent deformations by properly taking into account the NAPTF trafficking data and the previous loading stress history effects. A comparison of the measured and predicted permanent deformations indicated that a good match for the measured rut magnitudes and the accumulation rates could be achieved only when the magnitudes and variations of stress states in the granular layers, number of load applications, gear load wander patterns, previous loading stress history effects, and trafficking speed or loading rate effects were properly accounted for in the laboratory testing and permanent deformation model development.

KEY WORDS: Unbound aggregates, permanent deformation, testing and modeling, stress history, loading rate

1 INTRODUCTION

Rutting is the repeated load-induced permanent deformation of a flexible pavement. For pavement geomaterials, typically unbound base/subbase courses and subgrade soils, rutting is the only failure mechanism of relevance as no bound layers are involved. Unstabilized subgrade soils for low to medium volume roads and thick granular layers constructed for highway and airport flexible pavements are usually more susceptible to rutting damage. The recent European COST 337 project on unbound granular materials for road pavements highlighted the need to determine permanent deformation properties of unbound granular materials as a high priority, urgent research topic (Huhtala, 2002). To adequately assess the rutting potential of thick granular layers, it is important to properly apply in the laboratory actual field loading conditions including the effects of previous loading stress history, wheel load magnitudes, trafficking speed or loading rates, and continuously varying dynamic stress states due to moving wheel loads. These important aspects can be studied in the laboratory only by using advanced triaxial testing devices having the capability to apply constant and variable confining pressure (CCP and VCP) type stress path loadings to also simulate the rotation of principal stress directions and the extension and compression stress states induced by moving wheel loads (Kim and Tutumluer, 2005).

This paper summarizes research findings on characterizing and predicting the permanent deformation behavior of the P209/P154 granular base and subbase materials used recently in the construction and testing of the first round of flexible pavement test sections at the Federal Aviation Administration's (FAA's) National Airport Pavement Test Facility (NAPTF). A comprehensive laboratory study at the University of Illinois included conducting repeated load triaxial tests at various static and dynamic stresses under both CCP and VCP conditions. This paper, however, primarily focuses on the CCP test results, which represent mainly the field conditions realized directly under the wheel where the highest applied stress ratios are experienced in the granular layers and, as a result, the highest vertical permanent deformations are commonly recorded (Kim and Tutumluer, 2005). Rutting models developed based on these test results are presented and compared for prediction performances to identify primary factors affecting laboratory rutting evaluation of the NAPTF granular layers, i.e., the applied wheel load magnitude, number of load applications, gear load wander patterns, previous loading stress history effects, and trafficking speed or loading rate effects.

2 FULL-SCALE AIRPORT PAVEMENT TESTS AT FAA'S NAPTF

In the United States, the Federal Aviation Administration's (FAA's) National Airport Pavement Test Facility (NAPTF) was completed and dedicated in April 1999 to represent the most carefully constructed facility ever conceived for evaluating airport pavements (http://www.airtech.tc.faa.gov/NAPTF/). The NAPTF had 9 pavement test items built on three different low, medium, and high strength subgrade soils. There were six flexible pavement and three rigid pavement test items. Both P209 granular base and P154 granular subbase materials were extensively used in the construction of flexible and rigid pavement sections.

The NAPTF was constructed to generate full-scale testing/trafficking data to support the investigation of the performance of airport pavements subjected to complex gear loading configurations of new generation aircraft. Two gear configurations, a six-wheel tridem landing gear in one lane (representing the Boeing 777 aircraft gear) and a four-wheel dual-tandem landing gear in the other lane (representing the Boeing 747 aircraft gear) were tested simultaneously with an applied transverse wander pattern consisting of a fixed sequence of 66 vehicle passes (33 traveling East and 33 traveling West), as shown in Figure 1, arranged in 9 equally spaced wander positions (or tracks) at intervals of 0.26 m. Individual pavement dynamic response data were collected due to passing of each gear for various combinations of applied load magnitudes, traffic directions, and wander positions. To minimize the interaction of gear loads at the subgrade level, the four-wheel and six-wheel gears moved in phase, with both gears moving left and right together rather than towards and away from each other. Sensor installation included multi depth deflectometers (MDDs), the locations of which are shown for wander positions in Figure 1, and pressure cells to capture pavement responses under traffic loading. Rutting was monitored throughout the traffic test program by transverse surface profile measurements, rolling inclinometer and straightedge rut depth measurements, and individual layer rut data collected using MDDs.

Trafficking of the constructed pavement test sections was completed in 2001. Flexible pavement section distress/failure was indicated mainly by rutting of up to 100 mm permanent deformations observed on the surface. As is the case for most airfield pavements, the NAPTF flexible pavements test sections were designed to primarily fail in an excessive subgrade rutting type failure. In these pavements, however, considerable amount of rutting, determined from MDD data and test section forensic analyses, was found to take place in both P209 base and P154 subbase layers (Garg, 2003).

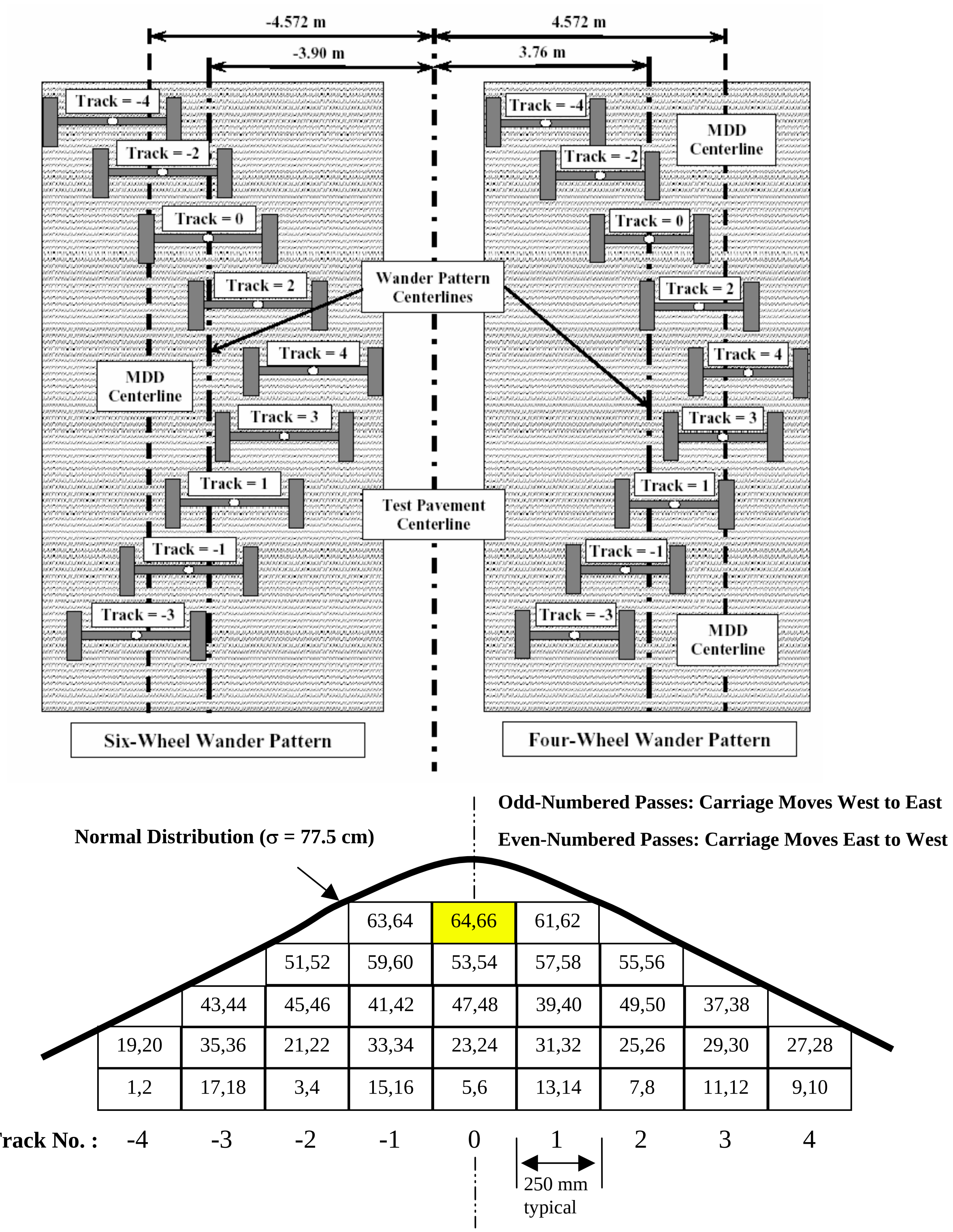

Figure 1: Applied traffic wander patterns and wander distributions in the NAPTF tests

The NAPTF flexible pavements constructed on the low strength (CBR=4) subgrades, low strength flexible conventional (LFC) and low strength flexible stabilized (LFS), were also the ones that had the thickest P209/154 granular base/subbase layers with the highest rut contributions in the pavement structure. The typical LFC and LFS pavement cross-sections and their nominal layer thicknesses are illustrated in Figure 2. The LFC and LFS sections were deemed to be the most challenging in rutting predictions and, therefore, utilized for field performance validation and calibration of the permanent deformation models developed in this study. In the low strength flexible conventional (LFC) section, the major contribution to permanent deformation was from the 914-mm thick P154 subbase at the wheel loads of 20.4 tonnes for the first 20,000 passes. After then, the wheel loading was increased to very high 29.5 tonnes and the permanent deformations increased significantly especially in the subgrade soil. The traffic speed was set at 8 km/h.

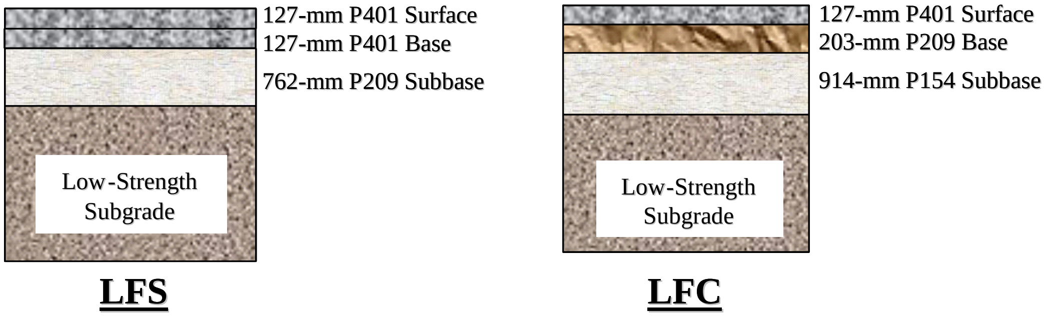

Figure 2: The NAPTF pavement cross-sections of LFS and LFC test sections

3 TESTING & MODELING FOR PERMANENT DEFORMATION

The FAA specified granular base and subbase materials P209 and P154, both crushed aggregate, were selected for permanent deformation testing using an advanced repeated load triaxial testing device previously introduced and referred to as the UI-FastCell (Tutumluer and Seyhan, 1999). The P209 base material is classified as A-1-a according to AASHTO procedure and as GP-GM according to ASTM procedure, whereas, the P154 subbase aggregate is classified as A-1-b according to AASHTO procedure and as SW-SM according to ASTM procedure. For the P209 and P154 materials, 7.5 mm and 1.7 mm are the average sizes, D_{50}, 19 mm and 37 mm are the top sizes, and 8% and 12% are the percentages passing No. 200 sieve size (0.075 mm), respectively. The modified Proctor (AASHTO T180) tests gave maximum dry densities of 24.2 kN/m^3 and 20.5 kN/m^3 for the P209 and P154 aggregates, respectively, corresponding to the optimum moisture contents of 5.1% for the P209 base and 6.5% for the P154 subbase materials. The P209 had a high friction angle of 61.7 degrees with cohesion of 132 kPa, whereas, the friction angle and cohesion intercept for the lower quality P154 were determined to be 43.9 degrees and 182 kPa, respectively.

3.1 Advanced Laboratory Test Program

A total of 4 stress path tests, 1 CCP and 3 VCP, were conducted on the crushed aggregate samples for the selected constant stress path slopes at four different static mean pressures (Kim and Tutumluer, 2005). In the CCP tests, different magnitudes of vertical wheel load stresses were repeatedly applied on laboratory specimens under constant confining pressures σ_3. The VCP repeated load triaxial tests, on the other hand, offer much wider loading possibilities by cycling confining pressure in phase with the axial deviator stress to simulate varying dynamic stress states that typically occur in the field under moving wheel loading. Nonetheless, this paper primarily focuses on the field conditions realized directly under the wheel where the highest applied stress ratios are also experienced in the granular layers and the highest permanent deformations are often recorded (Kim and Tutumluer, 2005).

Table 1 shows the typical CCP stress states used to evaluate the effects of applied stress magnitudes and stress ratios on the permanent deformation accumulation. The permanent deformation accumulation typically increases as the stress ratio increases and the confining pressure decreases (dilation effects) directly under the wheel load. As such, it is required to realistically consider: (1) relatively high stress magnitudes in airport granular layers under heavy aircraft gear loads (heavier than highway load magnitudes) and (2) stress ratios, σ_1/σ_3, as high as 10, where σ_1 is the total vertical stress and σ_3 is the total horizontal stress, acting on a representative pavement element. In permanent deformation testing, each deviator stress σ_d (= σ_1-σ_3) and confining pressure σ_3 pair, often referred to as a stress state shown in Table 1, was applied on different P209/P154 specimens with the deviator stress σ_d repeatedly pulsed for a total of 10,000 cycles to complete the test for a total of 13 permanent deformation tests conducted for each of the P209 and P154 materials.

Table 1: Permanent deformation testing stress states applied on the P154 and P209 aggregates

Stress Ratio $\sigma_1/\sigma_3 = 4$		Stress Ratio $\sigma_1/\sigma_3 = 6$		Stress Ratio $\sigma_1/\sigma_3 = 8$		Stress Ratio $\sigma_1/\sigma_3 = 10$	
σ_d (kPa)	σ_3 (kPa)	σ_d (kPa)	σ_3 (kPa)	σ_d (kPa)	σ_3 (kPa)	σ_d (kPa)	σ_3 (kPa)
62.1	20.7	96.6	20.7	144.9	20.7	186.3	20.7
103.5	34.5	172.5	34.5	241.5	34.5	310.5	34.5
165.6	55.2	276.0	55.2	386.4	55.2	*	*
207.0	69.0	345.0	69.5	*	*	*	*

*: could not be applied due to high stress states and test equipment limitation.

3.2 Permanent Deformation Model Development

A permanent strain database, consisting of 3250 stress-strain data sets, was formed for each of the P209 and P154 materials from all the CCP tests run at 13 stress states. The objective was to develop a model to best describe the permanent deformation behavior of P209 and P154 aggregates with the number of load repetitions and the applied static/dynamic stress states. Various mathematical forms such as linear, nonlinear, logarithmic, hyperbolic, were investigated using multiple regression analyses. Considering the typical exponential growth of permanent strains with number of load applications (N) in the triaxial tests, the power or logarithmic functions were found to be the most suitable as listed in Table 2.

Table 2 compares the regression correlation coefficients (R^2s), i.e., the goodness of the statistical fit, obtained for the 4 models. Model 4 was by far the best one giving the highest correlation coefficients. This model properly considered the effects of two independent applied stresses, deviator stress (σ_d) and confining pressure (σ_3) in the definition of the bulk stress ($\theta=\sigma_d+3\sigma_3$), and the number of load repetitions (N). With the bulk stress θ term used in the model instead of σ_3, Model 4 was also better applicable to implementing into finite element analysis for computing stress states in the granular layer directly under the wheel at the centerline of loading. It was therefore chosen as the most appropriate for predicting permanent strain/deformation accumulation for the P209 and P154 aggregates under various CCP stress states. Note that none of the 4 models given in Table 2 take into account the variable confining pressure (VCP) stress states and the effects of moving wheel loading conditions (see Kim and Tutumluer, 2005).

Table 2: Permanent strain models developed from P209 and P154 test data†

Materials	Regression Correlation Coefficient (R^2)	
	P209	P154
Model 1 : $\varepsilon_p = A*\sigma_3^B*N^C$	0.03	0.04
Model 2 : $\varepsilon_p = A*\sigma_d^B*N^C$	0.50	0.42
Model 3 : $\varepsilon_p = A*(\sigma_1/\sigma_3)^B*N^C$	0.62	0.78
Model 4 : $\varepsilon_p = A*\sigma_d^B*\theta^C*N^D$	0.86	0.85

†: A, B, C, and D are parameters for different models obtained from regression analyses.

4 MODEL VALIDATION WITH NAPTF DATA

For validating the newly developed CCP models, essentially Model 4, using the NAPTF trafficking field data, individual rut accumulations in the granular layers had to be predicted accurately with the increasing number of load applications (or number of wheel passes). This necessitated the estimation of the most accurate stress distributions in the P209/P154 granular layers to use as input in the permanent deformation models. Two finite element programs, ILLI-PAVE (Raad and Figueroa, 1980) and GT-PAVE (Tutumluer, 1995), were used to analyze NAPTF LFC and LFS pavement test sections to compute as accurately as possible the field stress states acting in the P209/P154 granular layers under the 20.4-tonne single wheel loading of the six-wheel and four-wheel gears. Both ILLI-PAVE and GT-PAVE programs consider the nonlinear stress dependent modulus behavior of granular bases and subgrade soils. The ILLI-PAVE and GT-PAVE finite element solutions predicted considerably high granular layer stress states, for example, vertical stresses as high as 510 kPa in the LFC P154 subbase layer. Note that such high stresses approach closely the strength properties of these unbound aggregate materials, which can explain the excessive shake down and permanent deformations took place in the P209/P154 layers as reported in the NAPTF tracking data.

Figure 3 shows accumulations of deformations computed in the P154 granular subbase layer of the LFC pavement test section due to the 9 different wander positions, or “tracks” assigned, of the 4-wheel gear. The measured LFC P154 layer rut accumulation is also shown in Figure 3 at the MDD centerline location (see Figure 1). First, average stress states were estimated for each track at mid-depth of the P154 subbase due to the superposition of 4 wheels and used as inputs to Model 4. The predicted permanent strain for each wander position or track was then multiplied by the total thickness of the P154 layer to compute the track permanent deformation accumulation as shown in Figure 3. Note that out of a complete wander sequence of 66 vehicle passes, the 9 wander positions or tracks of the 4-wheel gear were prorated for computing the number of load applications. For example, Track 0 (see Figure 1) had 10 passes while Track 3 had only 6 passes of the gear in a complete 66-pass wander sequence. In contrast, the x-axis in Figure 3 shows the actual total 20,000 passes of the gear with load wander, i.e., nearly 303 of the 66-pass complete wander sequence.

Figure 4 compares the NAPTF trafficking field data at the MDD centerline location (see Figure 1) with the total permanent deformations predicted for the LFC P154 subbase layer. The NAPTF measured ruts in the LFC P154 subbase layer accumulated with the number of wheel passes due to the 9 wander positions. There are two main differences between measured and predicted ruts shown in Figure 4: (1) the accumulation of actual ruts is following a linear trend rather than the power function curve predicted by Model 4 and (2) the predicted one gives somewhat higher rut accumulations, especially in the first cycle, compared to the measured NAPTF data for the LFC P154 subbase layer.

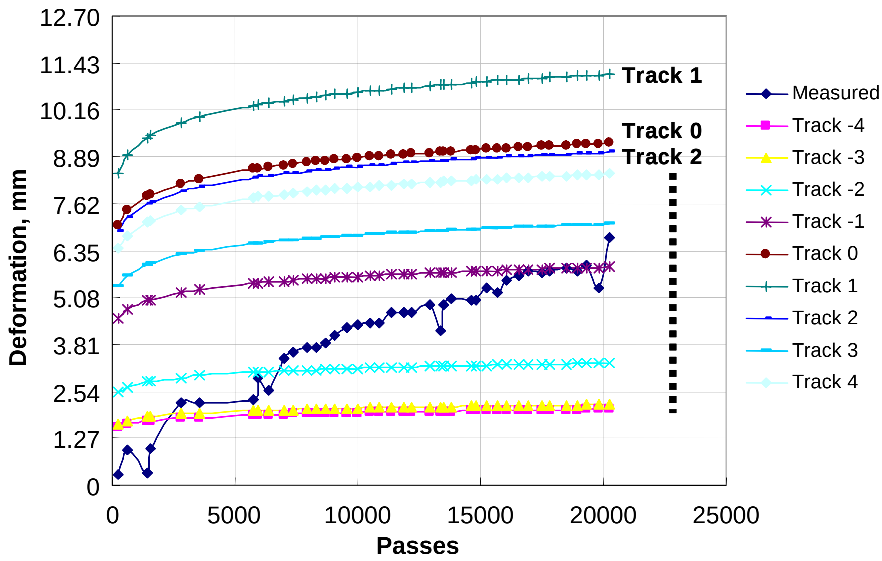

Figure 3: Individual wander position (or track) permanent deformations predicted at the MDD centerline location in the LFC P154 subbase layer

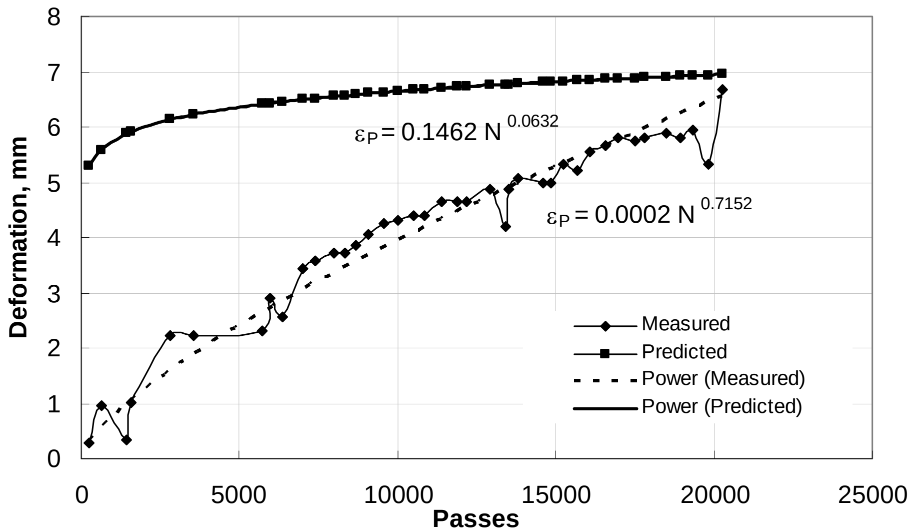

Figure 4: Measured and predicted permanent deformations in the LFC P154 subbase layer

4.1 Prediction Model Parameter Analysis

It has been customary and best fit from regression analyses to use a power function curve given by the equation $\varepsilon_p = A*N^B$ to establish the relationship between the laboratory measured permanent deformations and the number of load applications. In this equation, 'ε_p' is the permanent axial strain, 'N' is the number of load applications at that stress state, and finally, 'A' and 'B' are the model parameters obtained from regression analyses. In terms of the model parameters 'A' and 'B', the salient points of difference between the trend lines are highlighted in Figure 5. The measured P154 rut accumulation has a much larger 'B' value and a smaller 'A' value, compared to the model parameters of the predicted trend line (see Figure 4). In general, it is known that 'A' is quite related to the magnitude of permanent deformation due to the first load cycle, and 'B' is the slope of deformation accumulation line inversely proportional to the magnitude of the permanent deformation at the first load cycle.

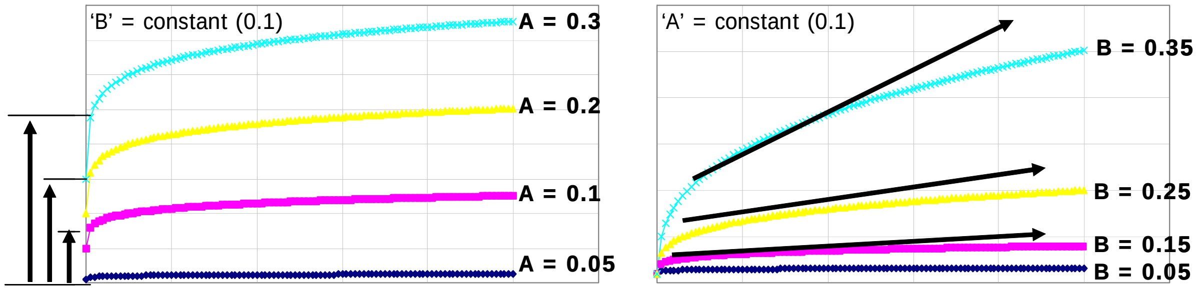

Figure 5: Effects of 'A' and 'B' parameters on the $\varepsilon_p = A*N^B$ power function type model

Analyzing the results, it was first realized that the load duration applied in the repeated load triaxial tests was not in accordance with the NAPTF trafficking speed. The permanent strain models were developed based on specimen testing at 0.1-second load duration, which corresponded to 48 km/h NAPTF vehicle speeds, whereas, the NAPTF sections were tested under 8 km/h gear loading equivalent to 0.5-second or longer load duration in the laboratory according to Barksdale (1971). To further investigate this effect of load duration, two additional P154 specimens were tested at a confining pressure of 21 kPa. The first one was tested under 63-kPa axial pulse loading with 0.1-second load duration, and after 72,000 cycles, the repeated stress level was increased to 336 kPa for another 72,000 cycles. The second specimen was pulsed with 0.5-second load duration at the same stress levels and number of load cycles as the previous one. As shown in Figure 6, the loading due to 0.5-second load duration accumulated approximately 40% more permanent deformations in the specimen than the 0.1-second load duration did. Hence, the load duration applied to specimens during testing has to be chosen in accordance with the field trafficking speed.

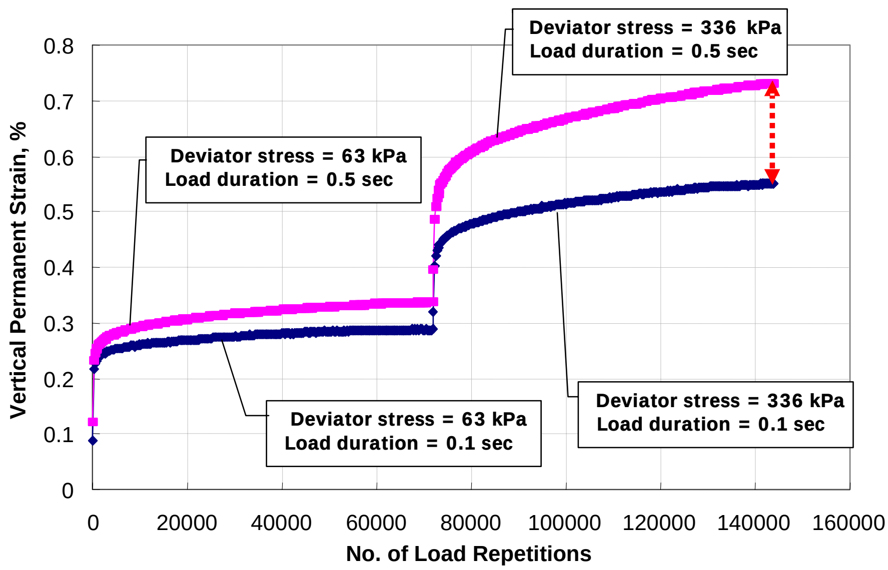

Figure 6: Illustration of load duration effect on the specimen permanent strain accumulation

Secondly, the specimens tested in the laboratory were not conditioned, whereas, the NAPTF pavement test sections had accumulated conditioning and stress history effects during the previous construction and response testing stages; especially when the slow moving response tests applied gear loadings up to 16.3 tonnes at the 0.54 km/h speed of the 4-wheel and 6-wheel assemblies. The P154/P209 base and subbase layers were certainly conditioned under these rather heavy loads applied during the slow moving response tests.

Three different P154 specimens were prepared and tested in the laboratory at the constant confining pressure of 21 kPa to investigate the so-called stress history effects on the P154 aggregate permanent strain behavior. Specimen 1 was not conditioned, whereas, specimens 2 and 3 were applied initial pulsed vertical stresses of 105 kPa and 336 kPa, respectively. Then, all three specimens were loaded at a dynamic vertical stress of 336 kPa. Figure 7 shows the test results with the 'A' parameter, which is the deformation at the first cycle, drastically increasing for the unconditioned virgin specimen and decreasing down to almost insignificant levels for the heavily conditioned third specimen. Also, the considerably higher value of the 'B' parameter in the power function model can be clearly seen in the heavily conditioned third specimen. Therefore, the small 'A' and the large 'B' parameters seen in the measured permanent deformation trends of the NAPTF granular base/subbase layers can be clearly linked to the stress history effects.

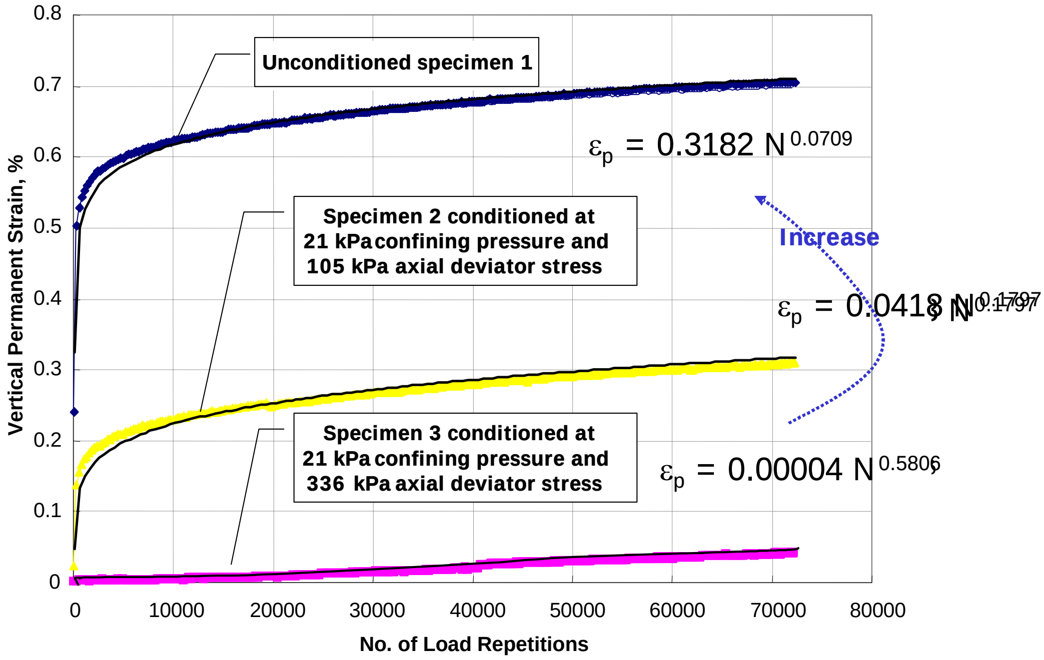

Figure 7: Illustration of stress history effect on the specimen permanent strain accumulation

Similar observations to those shown in Figures 6 and 7 were also reported by French researchers (El abd et al., 2004). Figure 8 shows predicted and measured unbound aggregate permanent strains with indications of stress history effects. The experimental findings represented by data points indicate more of linear type permanent deformation accumulations as stress levels increase for about three times. In other words, as stress history builds up in a specimen, the trend of permanent strain/deformation accumulation becomes more linear type, similar to the NAPTF full scale testing granular base/subbase permanent deformation trends.

5 SUMMARY & CONCLUSIONS

The U.S. Federal Aviation Administration's (FAA's) National Airport Pavement Test Facility (NAPTF) rutting performance data were utilized for the low strength subgrade flexible pavement test sections to validate permanent deformation models developed for the granular base and subbase layers, designated as P209 base and P154 subbase materials according to FAA's construction specifications. The functional form of the prediction models chosen for rutting performance analysis properly considered the effects of stress states applied on specimens under constant confining pressure type laboratory testing, field applied load wander patterns, and the number of load repetitions. Using the models, the maximum rut accumulations were predicted in the granular layers of the NAPTF low strength pavement test sections at 20,000 vehicle passes. In general, the magnitudes of permanent deformations were better predicted than the rates of permanent deformation accumulation with number of load applications. This was primarily due to the fact that the prediction models and their functional forms were developed based on the laboratory test data, which did not reflect the effects of stress history and load duration or traffic speed in the field. A better understanding of the field rut development under moving wheels and load wander patterns requires considerations of the stress history and load duration effects in full scale testing.

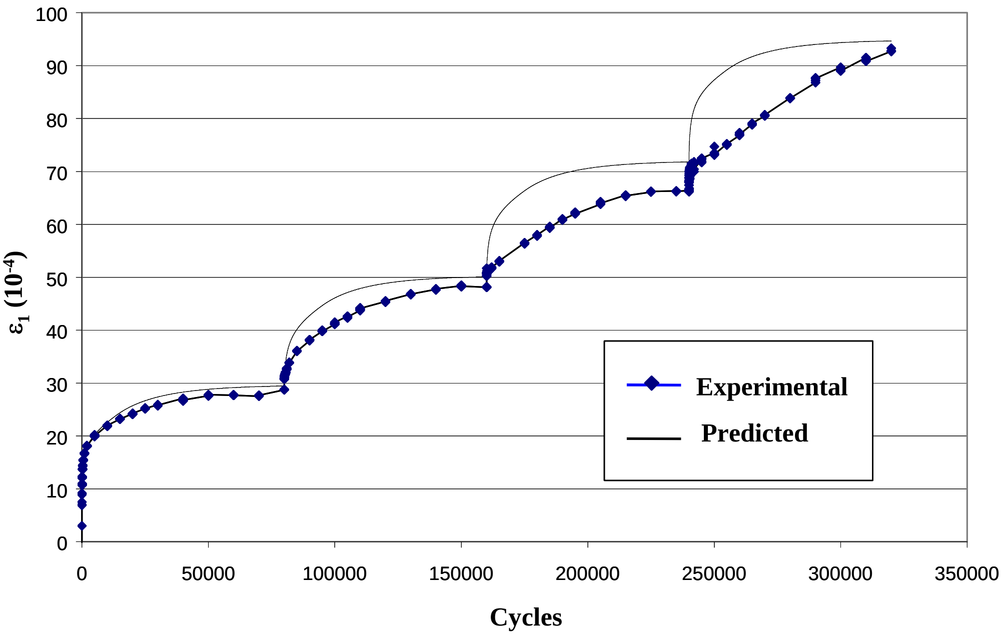

Figure 8: Predicted and measured unbound aggregate permanent strains (El abd et al., 2004)

REFERENCES

Barksdale, R. D., 1971. *Compressive Stress Pulse Times in Flexible Pavements for Use in Dynamic Testing*. Highway Research Record 345, Highway Research Board.

Garg, N., 2003. *Permanent Deformation Behavior of the Granular Layers Tested at the National Airport Pavement Test Facility*, Presented at the 82nd Annual Transportation Research Board Meeting, Washington, D.C. (http://www.airtech.tc.faa.gov/NAPTF/Download/)

El abd, A., Hornych, P., Breysse D., Denis, A., Chazallon, C., 2004. *A Simplified Method of Prediction of Permanent Deformations of Unbound Pavement Layers*, Proceedings of the 6th International Symposium on Pavements Unbound (UNBAR6), Nottingham, England.

Huhtala, M., 2002. *COST 337 – Unbound Granular Materials for Road Pavements,* Proceedings of the 6th International Conference on the Bearing Capacity of Roads, Railways, and Airfields, Lisbon, Portugal.

Kim, I.T., and Tutumluer, E., 2005. *Unbound Aggregate Rutting Models for Stress Rotation and Effects of Moving Wheel Loads*. In Proceedings CD-ROM of the 84th Annual Meeting of the Transportation Research Board, Washington, DC, January.

Raad, L., and Figueroa, J.L., 1980. *Load Response of Transportation Support Systems*, Journal of Transportation Engineering Division, ASCE, Vol. 106, No. TE1, January.

Tutumluer, E., 1995. *Predicting Behavior of Flexible Pavements with Granular Bases*, Ph.D. Dissertation, Georgia Institute of Technology, Atlanta, Georgia.

Tutumluer, E., and Seyhan, U., 1999. *Laboratory Determination of Anisotropic Aggregate Resilient Moduli Using A New Innovative Test Device.* Transportation Research Record 1687, Journal of the Transportation Research Board, National Research Council, Washington, DC, pp. 13-21.